The first-principles and ab initio molecular dynamics simulations revealing the interface energy of the NbC/α-Fe

Y. Li [a,b,d], J.H. Xu [c], W. Chen [a,b *], Y. Chen [d], F.J. Sun [a,b], L.G. Zhu [e], Q.J. Zhang [a,b,d], Y.K. Li [a,b], S. Chen [a,b]

[a]*College of Metallurgy and Energy, North China University of Science and Technology, Tangshan 063009, Hebei Province, China*
[b]*Hebei Province High-Quality Steel Continuous Casting Engineering Technology Research Center, North China University of Science and Technology, Tangshan 063210, Hebei Province, China*
[c]*Department of Chemistry, University College London, London WCE 6BT, England*
[d]*Comprehensive testing and analyzing center, North China University of Science and Technology, Tangshan 063009, Hebei Province, China*
[e]*School of Material Science and Engineering, Hebei University of Science and Technology, Shijiazhuang 050018, Hebei Province, China*

The low index interfacial configuration, interface energy and electronic properties of NbC/α-Fe are calculated using the first-principles method based on density functional theory and ab initio molecular dynamics simulation. Additionally, the NbC/α-Fe interface with the low index interfacial configuration is calculated by two-dimensional disregistry method. It is demonstrated that the Fe-C type has an interface energy of -1.553 J/m^2, the smallest interface energy and the most stable structure, therefore the Fe-C type is the most stable conformation of the NbC(001) /α-Fe(001). Strong orbital resonance phenomenon exists between Fe-3d, Nb-4d and C-2p, producing strong metallic and covalent bonds. The results of disregistry calculation by different interfacial structures of NbC/α-Fe shows that the disregistry of NbC(001)/α-Fe(001) crystalline surface is the smallest at 10.19%, which corresponds to the results of interface energy calculation. It can be shown that the α-Fe(001) is the optimal orientation surface of the NbC(001) . Herein, we have revealed the site-oriented and stable bonding mode relationship of NbC/α-Fe interface in steel, which provides important theoretical guidance to explore the mechanism of grain refinement of NbC particles in shipbuilding steels.

(Received December 17, 2023; Accepted April 1, 2024)

Keywords: NbC, First-principles calculations, Ab initio molecular dynamics simulation, Interface energy

1. Introduction

Transition metal niobium is a strong carbon-nitrogen forming element, exhibiting a strong tendency to form carbon-nitrides, which often precipitate as carbon-nitrides in steel[1]. NbC, as an important rock salt type transition metal carbide, has high melting point, super hardness and

* Corresponding author: hblgdxzzb@163.com
https://doi.org/10.15251/DJNB.2024.192.475

excellent chemical stability [2]. NbC has high thermal stability and is often used in metal heat treatment processes to prevent austenite grain boundaries from expanding by using undissolved NbC inclusions to pin down austenite grain boundaries during heating, which can play a role in fine grain strengthening[3-4]. NbC compounds have short bond lengths and ultra-hardness, and are widely used as alloy strengthening phases in cemented carbides[5]. The above properties are macroscopic properties of inclusions in steel, while their nano-scale properties have rarely been reported.

In recent years, the first-principles method[6-8] have made breakthroughs in various aspects of materials design, solving many problems that are difficult to explain experimentally, and playing an extremely important role in the study of bulk phases, surfaces and interfaces of compounds. It was reported that Schwarz[9] conducted a systematic study of the electronic structures of NbC and NbN and clearly resolved the energy band structure composition and charge density distribution between Nb atoms and C atoms in the forming NbC compounds. The surface energy, surface fold properties, charge density and density of states of NbC(001) surfaces were investigated by Huai-Zheng Zhang[10-11], and the surface energy was obtained by subtracting the bulk phase energy from the total energy of the flat plate. Liu et al.obtained that the NbC low index (001) surface is the most stable surface through simulations [12]. Yang[13] et al. calculated the surface energy of the NbC(111) surface and determined the minimum atomic layer thickness using the convergence of the surface energy. Wang, Haiyan et al. have simulated the structure of the interface between NbC particles and α-Fe in niobium-containing steel using first-principles approach[14]. The interface energy, charge density, density of states and overlap Bourget number of the interfacial configuration are analyzed in detail. Xiong[15]et al performed first-principles calculation for two bonding site configurations such as Fe-Nb and Fe-C at the NbC/α-Fe interface, where the results of the interfacial energy calculations were 5.84 J/m^2 and 4.54 J/m^2, indicating that the interfacial Fe-C bonding site configuration is more stable.

Meanwhile, the combination of first-principles calculation based on density generalized theory and ab initio molecular dynamics simulation has been widely used in materials science calculations. In the field of metallurgy, Johansson[16] et al. determined the energy and structure of the Fe(001)/VN(001) interface using ab initio molecular dynamic simulation methods. Wei [17] et al. calculated the adsorption and diffusion behavior of H_2S on ideal, defective and highly covered Fe(100) surfaces at 300 K using ab initio molecular dynamics for kinetic simulations. Wang [18] et al. used ab initio molecular dynamics methods to simulate and calculate the relaxation of Fe atoms adsorbed on the surface of TiN(001). It was found that the structural Fe atoms after relaxation all moved above the N atoms on the TiN(001) surface. The motion trajectories of Fe atoms on the TiN(001) surface were simulated and the charge transfer was analyzed in detail. Therefore, in order to achieve accurate control of steel solidification, inclusions precipitation and tissue refinement process, it is very necessary to use ab initio molecular dynamics method to conduct in-depth research on the nano nature and behavior of steel solidification tissue lattice structure, to obtain an accurate understanding of the solidification process change mechanism [19].

The interfacial bonding mode and bonding ability of NbC and α-Fe have a certain influence on the fine crystal strengthening effect. Due to the small size of the precipitated NbC particles, it is difficult to determine the interfacial relationship between them and α-Fe. Therefore, the properties of the NbC/α-Fe interface are investigated from a nano-view perspective using the first-principles and ab initio molecular dynamics methods. It helps to reveal the stable bonding mode and

site-directed relationship of NbC/α-Fe interface in steel, and provides a microstructural theoretical basis for exploring the grain refinement mechanism of NbC particles in shipbuilding steel.

2. Method of calculation

The calculations in this work were all performed with the first-principles based on density functional theory (DFT) and ab initio molecular dynamics simulation methods.The interface formed by NbC(001) and α-Fe(001) surfaces was selected for the study, and the NbC/α-Fe interface was constructed between the NbC(001) surface using a 5-layer atomic structure and the 5-layer structural α-Fe(001) surface based on the results of the previous surface property calculations [20]. The α-Fe(001) surface layer of Fe atoms bonded to the NbC(001) surface exists in three different positions, which are located above the Nb, bridge and C atoms, and the interface distance is chosen as 0.2 nm. Combined with the above bulk modulus calculation results, the bulk modulus value of NbC is 353 GPa and the bulk modulus of α-Fe is 143 GPa. α-Fe has a smaller bulk modulus and is easily stretched. Therefore, to accommodate the periodic boundary conditions inherent in supercell calculations, coherent interface relations are invoked by stretching the lattice length of the α-Fe(001) surface to accommodate the lattice of the NbC(001) surface.

Since three-dimensional periodic boundary conditions are used for the surface configuration, a vacuum layer of 1.2 nm is added above the surface along the Z-axis in order to eliminate interactions between different surface configurations and to allow free movement of atoms. In performing the interface calculations, the electron exchange correlation energy is corrected using the RPBE function in the generalized gradient approximation (GGA), the plane wave truncation energy is chosen to be 370 eV, the interaction between valence electrons and ionic real is described by the ultra-soft pseudopotential and the spin polarization is used in the interface calculations considering that the low-temperature ferrite is ferromagnetic.

Considering that the precipitation temperature of NbC particles is close to 1100 K, and the first-principles can only be calculated at the default temperature value of 0 K, which is not in line with the real situation. In order to better match the actual situation, the effect of temperature factor must be taken into account, and thus a temperature-controlled ab initio molecular dynamics simulation method is used to investigate in depth the interfacial configuration, bond length changes, and electronic structure. The calculation system is NPT, the temperature is 1100 K, the step length is 1 fs; the number of steps is 1000, and other parameters are selected with reference to the settings in the above interface first-principles calculation.

3. Results and discussion

The bulk phase properties of NbC and α-Fe crystal structures were calculated by structural optimization. From table 1, it can be indicated that optimized lattice constants agreed with the experimental results very well, which proves the accuracy of first-principles calculation, and provides a reliable theoretical basis for our calculation of the NbC/α-Fe interface.

Table 1. Computed and experimental value of the properties of NbC and α-Fe (Lattice constants 'a', Bulk modulus 'B_0' and Formation energies 'E').

System	Research	*A*/nm	*B*/GPa	*E*/eV
NbC	This work	0.44246	353	-1.27
	Ref.[21]	0.44930	307	-2.83
	Ref.[22]	0.44544	—	—
	Ref.[23]	—	—	-1.45
	Ref.[24]	0.45280	318	-2.06
α-Fe	This work	0.28377	143	—
	Ref.[25]	0.28664	—	—

3.1. The first-principles study of NbC(001)/α-Fe(001) structural relaxations:

The NbC(001)/α-Fe(001) interface structure is shown in Fig. 1 (Fig. 1(a) as an example, side view on the left; top view on the right), where Fig. 1(a) shows the initial NbC(001)/α-Fe(001) interface configuration with the Fe atom at the interface located above the Nb atom (denoted as Fe-Nb). Fig. 1(b) shows the initial configuration of the NbC(001)/α-Fe(001) interface with the Fe atom at the interface located above the bridge position (denoted as Fe-bridge). Figure 1(c) shows the initial configuration of the NbC(001)/α-Fe(001) interface with the Fe atom at the interface located above the C atom (denoted as Fe-C).

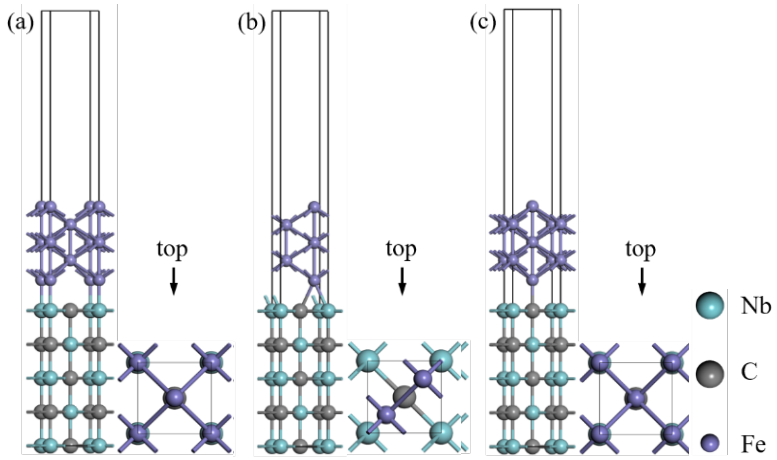

Fig. 1. Side and top views of the initial configuration of the NbC(001)/α-Fe(001) interface: (a)-Fe-Nb; (b)-Fe-bridge; (c)-Fe-C.

Fig. 2 shows the interfacial atomic configuration of the above three NbC(001)/α-Fe(001) after relaxed optimization. It can be seen that no surface reconfiguration occurred in any of the three interfacial configurations. In the NbC(001)/α-Fe(001) configuration of Fe-Nb type, the Fe atoms are located above the Nb atoms and no motion occurs in the cross section of the interface, while the α-Fe(001) atomic layer is shifted toward the vacuum layer in the vertical interface

direction, and the interfacial spacing increases by 0.0578 nm compared with the initial Fe-Nb configuration. In the Fe-bridge type NbC(001)/α-Fe(001) interface configuration, the Fe atoms at the interface slip in the cross-sectional direction and move above the C atoms, while moving toward the NbC(001) side along the vertical interface direction, where the interface spacing increases by 0.0133 nm compared to the initial Fe-bridge configuration. In the Fe-C type NbC(001)/α-Fe(001) interfacial configuration, the Fe atoms at the interface are located above the C atoms and no motion occurs in the interfacial cross section, while the α-Fe(001) atomic layer shifts toward the NbC(001) side of the interface in the vertical interfacial direction, where the interfacial spacing decreases by 0.0078 nm compared to the initial Fe-C configuration.

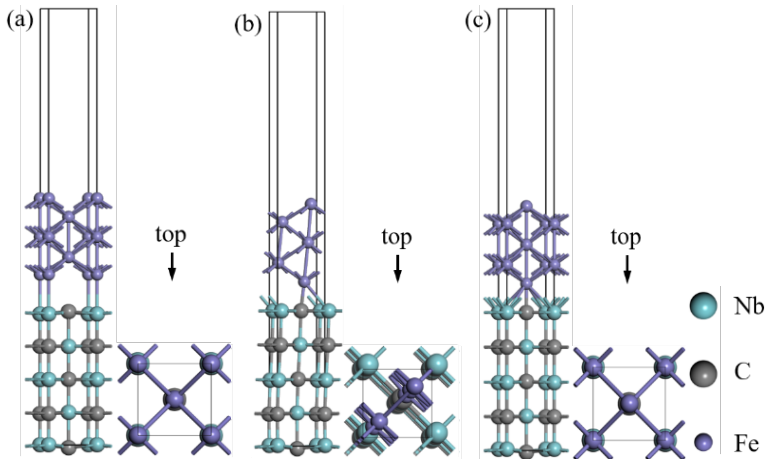

Fig. 2. Side and top views of the relaxation structure at the NbC(001)/α-Fe(001) interface: (a)-Fe-Nb; (b)-Fe-bridge; (c)-Fe-C.

By comparing the changes of the interfacial spacing of the three NbC(001)/α-Fe(001) configurations, it can be found that the interfacial spacing decreases in the other two except for the increase in the interfacial spacing of the Fe-Nb type structure. In the NbC(001)/α-Fe(001) conformational interface with Fe-bridge bonding mode, the Fe atom is more likely to move above the C atom, thus indicating that the Fe atom is more likely to bond with the C atom.

To evaluate the stability of the three structures, the interface energy was calculated for the structures following the equation in literature[26-27]. The system energies of the above surface and interface are calculated using the first- principles method for the structural single-point energy. The interface energy of the initial interfacial configuration NbC(001)/α-Fe(001) was calculated and the results are listed in Table 2. The minimum interface energy of Fe-C type structure is -1.553 J/m^2 and the most stable interface, the maximum interface energy of Fe-Nb type structure is 1.431 J/m^2 and the structure is unstable, and the magnitude of interface energy of Fe-bridge type structure is between the former two, indicating that the chemical bonding at this position is in a sub-stable state. This indicates that C atoms are more easily bonded to Fe atoms.

Table 2. Interface energy of NbC(001)/α-Fe(001) conformation.

Interface	Interface combination method	Interface energy /(J/m^2)
NbC(001)/α-Fe(001)	Fe-Nb	1.431
	Fe-bridge	-0.292
	Fe-C	-1.553

3.2. Ab initio molecular dynamics study of NbC(001)/α-Fe(001) interface:

The precipitation temperature of NbC particles is about 1100 K. The different conformations of NbC(001)/α-Fe(001) after ab initio molecular dynamics simulation relaxation, the structural morphology is shown in Fig. 3. It can be seen that the NbC(001)/α-Fe(001) conformational interface after relaxation does not undergo reconstruction, and the Fe-C-type interfacial structure quickly reaches a stable equilibrium state, while both Fe-Nb-type and Fe-bridge-type interfacial structures undergo interfacial cross-sectional slip motion. The Fe atom at the interface of NbC(001)/α-Fe(001) configuration eventually moves above the C atom on the NbC(001) face, which can indicate that the Fe-C type NbC(001)/α-Fe(001) interface structure is the most stable, and the C atom is the best bonding position for the Fe atom.

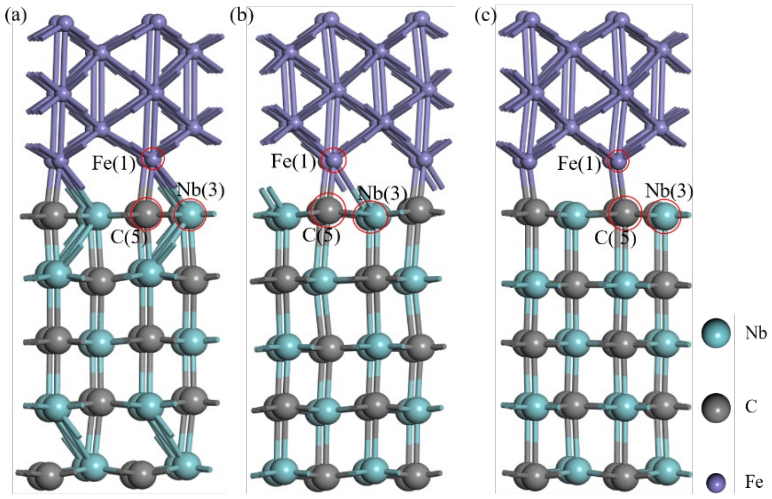

Fig. 3. Snapshot morphology of NbC(001)/α-Fe(001) interface relaxation conformation: (a)—Fe-Nb; (b)—Fe-bridge; (c)—Fe-C.

The interfacial spacing of the different initial configurations of the NbC(001)/α-Fe(001) interface after sufficient relaxation is listed in Table 3. The interfacial spacing of the NbC(001)/α-Fe(001) interfacial conformation is around 0.19 nm after structural relaxation, and the interfacial spacing is reduced compared with that of the initial conformation, which is consistent with the result that the Fe atoms are eventually shifted above the C atoms at the interfacial part of the conformation.

Table 3. Interfacial spacing after relaxation of NbC(001)/α-Fe(001) conformation.

Interface	Interface spacing /nm		
	Fe-Nb	Fe-C	Fe-bridge
NbC(001)/α-Fe(001)	0.194	0.189	0.195

To further analyze the motion process of the NbC(001)/α-Fe(001) interface, the variation of the chemical bond lengths between Fe(1) atoms and Nb(3) or C(5) atoms at the interface with time was used to reveal the mutual motion characteristics of the NbC/α-Fe interface, where the variation curves of the chemical bond lengths with time are shown in Fig.4.

From Fig. 4, it can be seen that the bond lengths of Fe(1)-C(5) bonds at the interface after relaxation of all three interfacial configurations fluctuate up and down at 1.9 Å and are always smaller than those of Fe(1)-Nb(3) bonds, which indicates that the Fe(1)-C(5) bonds are stronger and more stable. It shows that the C atom in the NbC/α-Fe interface is the best bonding position for the Fe atom.

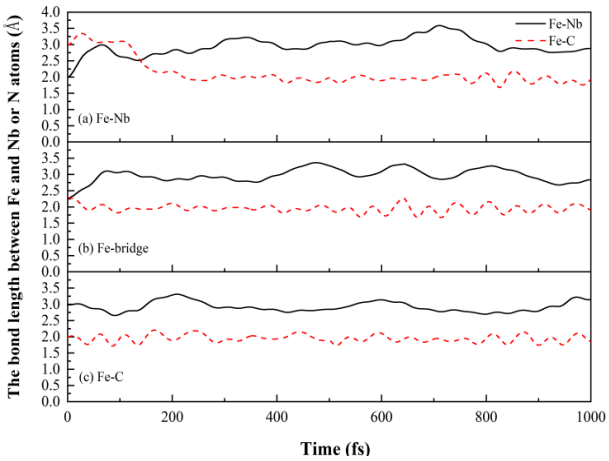

Fig. 4. Variation of bond lengths between Fe atoms and Nb and C atoms at the NbC(001)/α-Fe(001) interface with step size.

To further clarify the variation of bond lengths in Fig. 4, the effective charge transfer between atoms in the NbC(001)/α-Fe(001) interfacial configuration (see tables 4-6) was analyzed using the Mulliken charge layout analysis method. Throughout tables 4 to 6 the effective charge transfer amounts, except for the Fe-C type NbC(001)/α-Fe(001) structure, a large amount of charge transfer occurs at the interface of Fe-bridge type and Fe-Nb type NbC(001)/α-Fe(001) structures.

Table 4. Effective charge transfer at the Fe-Nb type NbC(001)/α-Fe(001) interface.

Number of layers /n	Atoms	Electric charge /e		Amount of charge transfer /e
		Unrelaxed	Relaxed	
3	Fe	-0.02	0.08	0.1
2	Fe	-0.23	-0.07	0.16
1	Fe	-0.06	0.14	0.2
1	Nb	1.05	0.62	0.43
	C	-0.64	-0.72	0.08
2	Nb	0.8	0.74	0.06
	C	-0.71	-0.68	0.03
3	Nb	0.73	0.73	0
	C	-0.71	-0.67	0.04

Table 5. Effective charge transfer at Fe-bridge type NbC(001)/α-Fe(001) interface.

Number of layers /n	Atoms	Electric charge /e		Amount of charge transfer /e
		Unrelaxed	Relaxed	
3	Fe	0.04	0.05	0.01
2	Fe	-0.05	-0.05	0
1	Fe	0.03	0.18	0.15
1	Nb	0.79	0.6	0.19
	C	-0.69	-0.7	0.01
2	Nb	0.77	0.68	0.09
	C	-0.7	-0.68	0.02
3	Nb	0.73	0.68	0.05
	C	-0.71	-0.68	0.03

Table 6. Effective charge transfer at Fe-C type NbC(001)/α-Fe(001) interface.

Number of layers /n	Atoms	Electric charge /e		Amount of charge transfer /e
		Unrelaxed	Relaxed	
3	Fe	0.11	0.09	0.02
2	Fe	0.02	-0.06	0.08
1	Fe	0.13	0.16	0.03
1	Nb	0.6	0.59	0.01
	C	-0.72	-0.69	0.03
2	Nb	0.73	0.68	0.05
	C	-0.7	-0.7	0
3	Nb	0.74	0.76	0.02
	C	-0.71	-0.7	0.01

The analysis shows that the bond length change before and after relaxation at the NbC(001)/α-Fe(001) interface is closely related to the charge transfer. Combining Fig. 4 with Tables 4 to 6, it can be seen that before and after the relaxation of the NbC(001)/α-Fe(001) interfacial configuration of Fe-Nb type, there is a large amount of charge transfer between Fe, Nb, and C atoms at the interface, and a large electrostatic repulsion between Fe atoms and adjacent Nb atoms, which drives a large increase in the Fe-Nb chemical bond bond length, and on the contrary, the electrostatic gravitational force between Fe atoms and C atoms increases, which in turn reduces the Fe-C chemical bond length. The Fe-bridge type of NbC(001)/α-Fe(001) interface has a large charge transfer, resulting in an increase in the Fe-Nb chemical bond bond length and a decrease in the Fe-C chemical bond length, with the transfer of the Fe atom from above the bridge to above the C atom. Before and after the relaxation of the NbC(001)/α-Fe(001) interface of Fe-C type, the effective charge transfer between Fe, Nb, and C atoms at the interface is smaller, which generates less electrostatic force and has less effect on the chemical bonding, and the Fe-Nb and Fe-C chemical bonds are more stable.

To clarify the bonding situation at the interface between NbC(001) and α-Fe(001), the partial density of state (PDOS) properties before and after the relaxation of their interfacial configurations were analyzed separately. The valence electron of Fe is $3d^6 4s^2$, and the subsequent analysis of the PDOS of Fe atoms is mainly performed using the higher energy Fe-3d orbitals. For the calculation of PDOS of Nb and C atoms, the same orbitals (Nb-4d, C-2s, C-2p) as the above mentioned NbC low index surface density of states are used Fig. 5 to 7 show the PDOS before and after relaxation for the three NbC(001)/α-Fe(001) configurations.

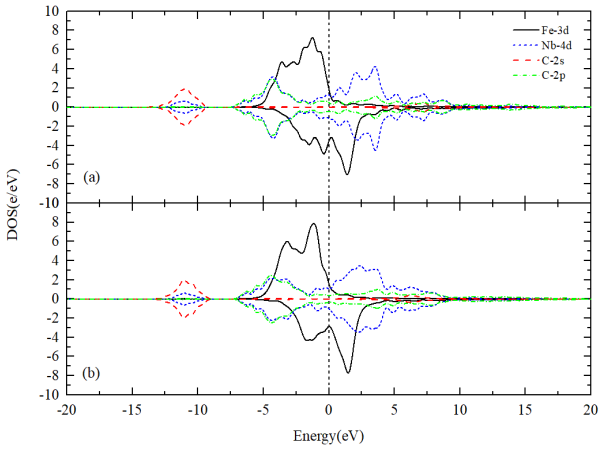

Fig. 5. PDOS for Fe-Nb type interface configuration (a) Unrelaxed, (b) Relaxed. The dotted line refers to the Fermi level.

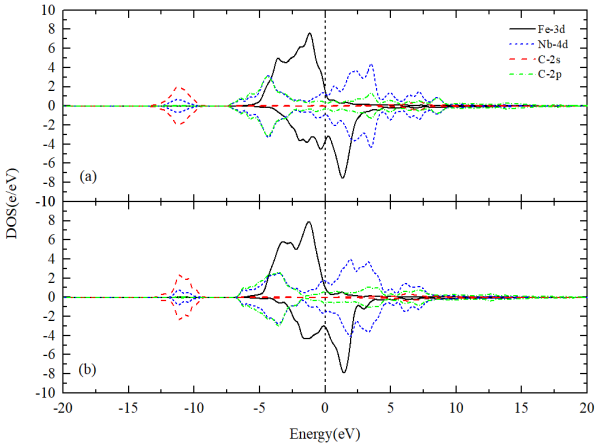

Fig. 6. PDOS for Fe-bridge type interface configuration (a) Unrelaxed, (b) Relaxed. The dotted line refers to the Fermi level.

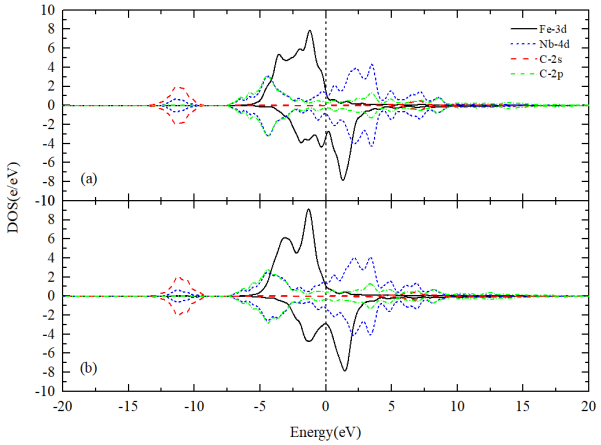

Fig. 7. PDOS for Fe-C type interface configuration (a) Unrelaxed, (b) Relaxed. The dotted line refers to the Fermi level.

We can find that the PDOS of Fe atoms is asymmetric in the upper and lower orbitals and exhibits extremely strong ferromagnetism, which requires consideration of the effect of spin polarization on the calculation, while the upper and lower orbitals of the spin fractional density of Nb and C atoms are almost symmetric, indicating that Nb and C atoms are not ferromagnetic and do not need to consider spin polarization. The Nb-4d and C-2p orbital energies in the bonding state after relaxation in all three configurations show a tendency to decrease and shift to the right compared to the corresponding orbital energies before relaxation, with new peaks near -3.3 eV for the Fe-Nb configuration, -3.5 eV for the Fe-bridge configuration, and -3.6 eV for the Fe-C configuration. The trends of Nb-4d and C-2p orbitals are roughly similar, and the orbitals obviously overlap, indicating a strong orbital hybridization between Nb-4d and C-2p orbitals, and the Nb-C chemical bond is extremely stable. The number of Fe-3d orbital peaks in all three configurations is reduced compared with that before relaxation, and there is a tendency for the orbital energy to shift to the left, forming a peak near 3.2 eV, indicating that there are strong orbital resonances between Fe-3d orbitals and Nb-4d and C-2p orbitals, leading to the formation of stronger metallic and covalent bonds.

3.3. Interfacial properties and disregistry between NbC/α-Fe low index surfaces

From the above NbC(001)/α-Fe(001) interface ab initio molecular dynamics simulation calculations, it is clear that the best bonding positions of Fe atoms on the α-Fe surface on the NbC(001) surface are above the C atoms. Therefore, the model constructed in this section only considers the Fe-C configuration, and the selected low-index surfaces for NbC include the (001), (110), and N terminatied (111) surfaces. The low index surfaces selected for α-Fe include (001), (110), and (111) surfaces. Due to the more stable Fe-C conformation, the step length of 1 fs was chosen for the ab initio molecular dynamics simulation and the number of steps was chosen to be 300. The model construction and calculations are all consistent with those in the NbC(001)/α-Fe(001) interface described above.

The initial configuration (left) and the post-relaxation configuration (right) of the NbC/α-Fe low index interfacial interface are shown in Fig.8, where the parallel crystallographic relations formed between NbC and α-Fe low index surfaces include: (a)NbC(001)/α-Fe(001), (b)NbC(001)/α-Fe(110), (c)NbC(001)/α-Fe(111), (d)NbC(110)/α-Fe(001), (e)NbC(110)/α-Fe(110), (f)NbC(110)/α-Fe(111), (g)NbC(111)/α-Fe(001), (h)NbC(111)/α-Fe(110), (i)NbC(111)/α-Fe(111).

From Fig. 8, it can be seen that the initial configuration of the NbC/α-Fe low index surface interface is relatively stable after relaxation, and (a)NbC(001)/α-Fe(001) interface structure is relatively stable without interfacial deformation and reconfiguration. However the α-Fe side of the (b)NbC(001)/α-Fe(110), (c)NbC(001)/α-Fe(111), (d)NbC(110)/α-Fe(001), (e)NbC(110)/α-Fe(110),(f)NbC(110)/α-Fe(111),(g)NbC(111)/α-Fe(001),(h)NbC(111)/α-Fe(110), (i) NbC(111)/α-Fe(111) interfacial configuration produces a severe reconstruction phenomenon. As a result, it can be concluded that (a) NbC(001)/α-Fe(001) is the optimal orientation relationship for NbC/α-Fe, which is consistent with the results of B-N orientation relationship obtained by Baker et al [28].

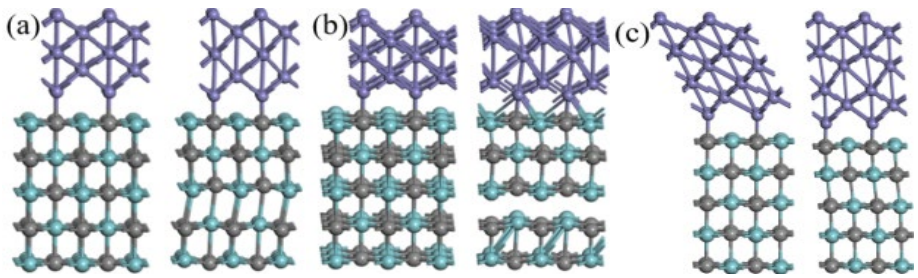

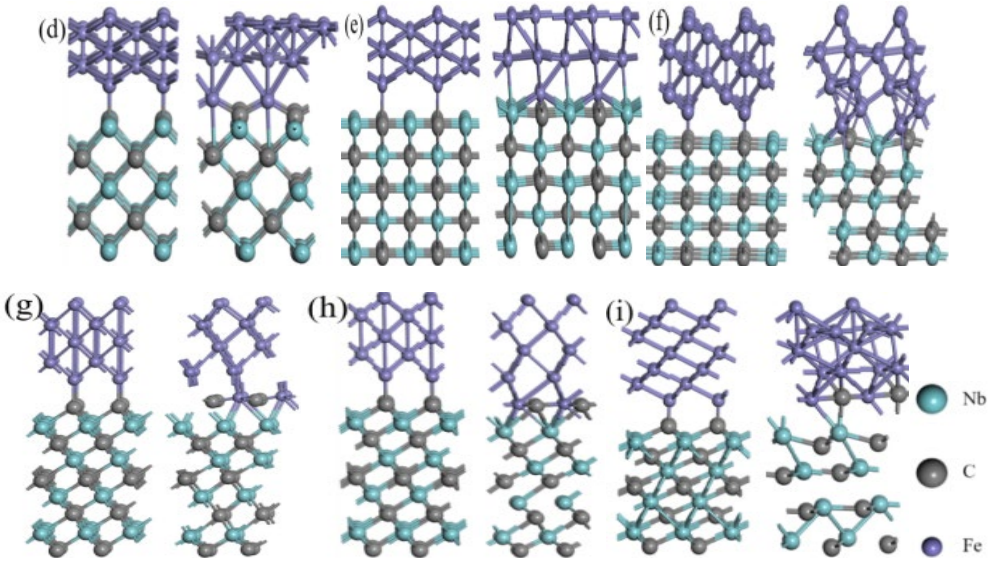

Fig. 8. Initial configuration of NbN/α-Fe low index interfacial interface (left) and post-relaxation structure (right) morphology.

The reason for the above phenomenon may be due to the large bulk modulus of NbC, and the α-Fe is influenced by the lattice coherence of NbC, so that the interfacial α-Fe side configuration is subsequently genetically deformed. Therefore, it can be seen that the structures on the α-Fe side of the interface configuration formed with the NbC(001) surface all produce a tendency to deform toward the (001) crystal-oriented structure, and the α-Fe(001) surface is the optimal orientation surface for the NbC(001) surface.

In order to further compare the stability of the interfacial structures between NbC/α-Fe low index surfaces, interfacial energy calculations were performed for the structures, and the results are listed in Table 7. We can find that the NbC(001)/α-Fe(001) interfacial energy is negative, and it is easier to form the interface and the interface is more stable. The NbC(001)/α-Fe(001) interface has an energy minimum of -1.553 J/m^2 in its system. It can be shown that the α-Fe(001) face has the best orientation relationship with the NbC(001) face, which is consistent with the above conformational relaxation results.

Table 7. Interface energy of NbC/α-Fe low index interfacial interface (J/m^2).

NbC low index surface	Interface energy with α-Fe(001)	Interface energy with α-Fe(110)	Interface energy with α-Fe(111)
(001)	-1.553	-0.928	3.884
(110)	5.679	6.092	1.443
C-term(111)	3.133	3.809	0.533

According to the conclusion drawn by Bramfitt, three sets of crystallographic orientations were selected for each set of parallel crystallographic relationships in the NbC/α-Fe low index interfacial structure, and the specific calculation was carried out for the NbC(001)/α-Fe(001)

parallel crystallographic relationship as an example, the lattice constants of NbC and α-Fe at 1100 K are 0.44464 nm and 0.28534 nm, respectively.

$$\delta_{\alpha\text{-Fe}(001)}^{\text{NbC}(001)} = \frac{|\frac{\sqrt{2}}{2}a_0 - b_0|}{b_0 \times 3} + \frac{|a_0 - \sqrt{2}b_0|}{\sqrt{2}b_0 \times 3} + \frac{|\frac{\sqrt{2}}{2}a_0 - b_0|}{b_0 \times 3} \quad (1)$$

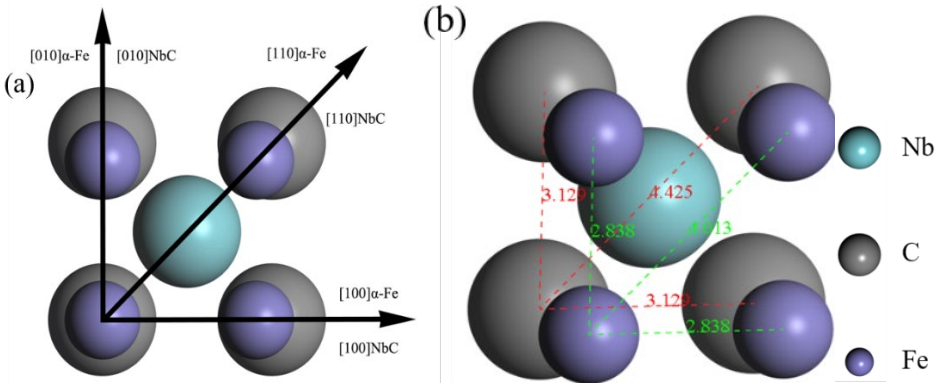

Fig. 9. Crystallographic relationship between NbC(001) and α-Fe(001) facets. (a)-Top view, (b)-Side view.

As shown in Fig. 9, the [010] crystal-oriented atomic spacing ds of the NbC(001) face is 0.3129 nm, which is equivalent to $\sqrt{2}$ times its lattice constant a_0. The atomic spacing d_n in the [010] crystal orientation of the α-Fe(001) surface is 0.2838 nm, which is equivalent to its lattice constant d_n, and the angle between the two crystal orientations is 0 degrees. The best matching atomic spacing d_s in the [110] crystal orientation of the NbC(001) face is 0.4425 nm, which is equivalent to its lattice constant a_0. The atomic spacing d_n in the [110] crystal orientation of the α-Fe(001) surface is 0.4013 nm, which is equal to $\sqrt{2}$ times its lattice constant b_0, and the angle between the two crystal orientations is 0 degrees. The [100] crystal-oriented atomic spacing d_s of the NbC(001) face is 0.3129 nm, which is equivalent to $\sqrt{2}$ times its lattice constant a_0. The atomic spacing d_n in the [100] crystal orientation of the α-Fe(001) face is 0.2838 nm, which is equivalent to its lattice constant b_0, and the angle between the two crystal orientations is 0 deg. The disregistry δ between the NbC(001) and α-Fe(001) crystal faces is 10.19.

Similarly, the disregistry degree of other parallel crystal surfaces between NbC and α-Fe crystal low index surfaces can be obtained, and the calculation results of the disregistry degree of parallel crystal surfaces are listed in Table 8.

Table 8. Disregistry between different low index surfaces of NbC and α-Fe at 1100 K (%).

NbC low index surface	Disregistry degree with α-Fe(001) surface	Disregistry degree with α-Fe(110) surface	Disregistry degree with α-Fe(111） surface
(001)	10.19	20.33	19.89
(110)	33.01	44.95	19.15
C-term(111)	11.65	21.19	22.09

According to Table 8, the disregistry values between NbC(001)/α-Fe(001) and NbC(111)/α-Fe(001) parallel crystalline surfaces are in the range of 6-12%, indicating that both have certain bonding ability, while the disregistry values between other parallel crystalline surfaces are greater than 12, and there is no mutual adhesion nucleation ability.

By analyzing the calculated results of the disregistry between the low index surfaces of NbC/α-Fe, it can be concluded that NbC(001)/α-Fe(001) is the best orientation relationship and is similar to the calculated results of NbC/α-Fe interfacial mismatch by Wang Yan et al [30], which corresponds to the above interfacial relaxation results and interfacial energy calculations and agrees well with the diffraction patterns obtained by Nayak et al [31-32].

3.4. Experimental verification

Based on DH36 steel produced by a factory in North China, the composition design of the test steel was carried out by adding an appropriate amount of microalloying elements. The four test tempering chemical components are shown in Table 9.

Table 9. Chemical composition of the DH36 steels (wt %).

Samples	C	Mn	S	P	N	Si	Al	Mo	Ti	Mg	V	Nb
1	0.12	1.00	0.007	0.02	0.0042	0.11	0.02	0.08	0.014	0.0005	0.005	0.003
2	0.09	1.0	0.007	0.02	0.0042	0.10	0.01	0.06	0.0006	0.0018	0.003	0.02
3	0.16	1.87	0.008	0.02	0.0042	0.40	0.05	0.07	0.003	0.0005	0.007	0.04
4	0.15	2.03	0.008	0.02	0.0042	0.40	0.12	0.07	0.01	0.001	0.007	0.06

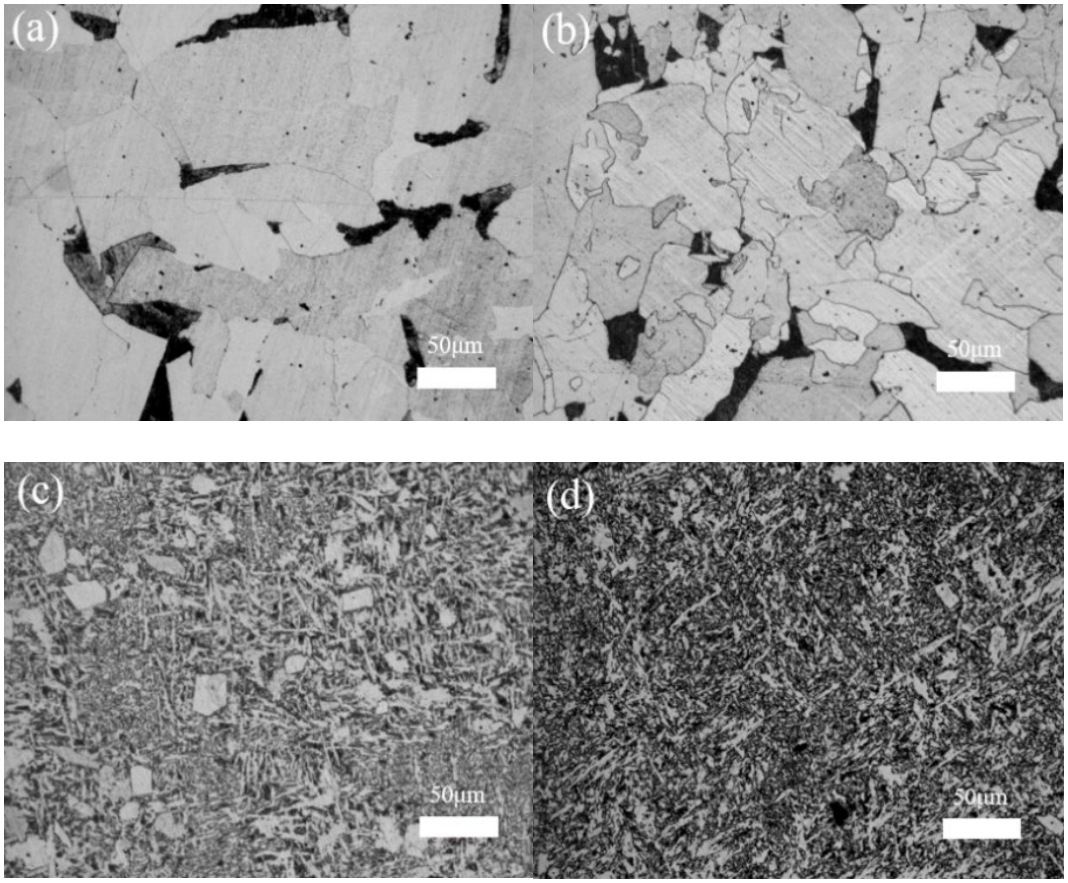

Fig. 10. Microstructure of DH36 steels with different Nb content at 200× magnification.(a)-0.003%, (a)-0.02%, (a)-0.04%, (a)-0.06%.

It can be seen from Fig.10, under the same magnification, the grain size gradually decreases with the increase of Nb content in the DH36 steel. Fig.10(a) shows the microstructure of the DH36 steel with Nb content of 0.003%, which is mainly composed of relatively coarse ferrite grains and pearlite grains, (b) shows the microstructure of the DH36 steel with 0.02% Nb content, which is mainly composed of ferrite and pearlite, with a certain number of fine intracrystalline ferrite grains, (c) shows the microstructure of the DH36 steel with Nb content of 0.04%, which is mainly composed of massive ferrite, acicular ferrite and bainite with relatively small grain size, (d) shows the microstructure of the DH36 steel with 0.06% Nb content, which is mainly composed of acicular ferrite, granular bainite and a small amount of equiaemic ferrite. The results show that the addition of Nb can refine the structure of steel matrix to a certain extent, improve the nucleation probability of intracrystalline ferrite, increase the precipitation amount of intracrystalline acicular ferrite, reduce the grain size, and then improve the strength and toughness of steel matrix.

4. Conclusions

In conclusion, the NbC/α-Fe low index interfacial structure has been simulated and optimized using first-principles calculation, ab initio molecular dynamics simulations and two-dimensional disregistry theory. The main results are summarized as follows:

The relaxation optimization of the NbC(001)/α-Fe(001) structure was carried out using the first-principles method, and the interface energies of Fe-Nb, Fe-bridge and Fe-C NbC(001)/α-Fe(001) structures were calculated to be 1.431 J/m^2, -0.292 J/m^2 and -1.553 J/m^2, respectively, indicating that Fe-C type is the most stable conformation of NbC(001)/α-Fe(001).

Conformational relaxation of the NbC(001)/α-Fe(001) structures was performed using ab initio molecular dynamics methods, and it was found that the Fe atoms at the conformational interfaces all moved above the C atoms after relaxation. It was found that the three NbC(001)/α-Fe(001) initial interfacial configurations were transformed into Fe-Nb-type and Fe-bridge-type NbC(001)/α-Fe(001) interfacial structures after sufficient relaxation, indicating that Fe-C-type is the most stable configuration. Meanwhile, the strong orbital resonance phenomenon exists between Fe-3d orbitals and Nb-4d and C-2p orbitals, producing strong metallic and covalent bonds.

The relaxation optimization of different interfacial structures of NbC/α-Fe using ab initio molecular dynamics method, and it was found that the interface energy of NbC(001)/α-Fe(001) interfacial structure was minimized to -1.553 J/m^2 and the interfacial configuration was the most stable. The results of disregistry calculations for different interfacial structures of NbC/α-Fe showed that the disregistry of NbC(001)/α-Fe(001) crystalline surface was the smallest at 10.19%, which corresponded to the results of interfacial energy calculations. It can be shown that the α-Fe(001) surface is the optimal orientation surface for the NbC(001) surface. This work reveals the stable bonding mode and site-directed relationship of NbN/α-Fe interface in steel, which has some theoretical guidance to explore the mechanism of grain refinement of NbC particles in shipbuilding steel.

Metallographic observation was carried out on four groups of DH36 steels with different Nb content. With the increase of Nb content in DH36 steels, the grain size gradually decreased, indicating that the addition of Nb element can play a certain refining role on the steel matrix structure, improve the nucleation probability of intracrystalline ferrite, increase the amount of precipitation of intracrystalline acicular ferrite, and reduce the grain size.The strength and toughness of the steel matrix can be improved.

Acknowledgements

This work is supported by the National Natural Science Foundation of China [grant numbers 51874137 and 51904107], Key project of National Natural Science Foundation of China-Joint Fund for Regional Innovation and Development [grant number U21A20114], and the Hebei Province Natural Science Fund [grant numbers E2020209036, 2020209005 and 2021209094].

References

[1] Deardo A J., International Materials Reviews, 2003, 48(6):371-402; https://doi.org/10.1179/095066003225008833

[2] Kan, Dongxiao, Zhang, Xilin, Zhang, Yanxing, Yang, Zongxian, Journal of Power Sources,2018,378:691-698; https://doi.org/10.1016/j.jpowsour.2018.01.014

[3] Yang Penghui, Fu Hanguang, Guo Xingye, Rachid Bennacer, Lin Jian, Journal of Materials Research and Technology,2020,9(3): 3109-3120; https://doi.org/10.1016/j.jmrt.2020.01.056

[4] M.G. Brik, C.G. Ma, Comput. Mater. Sci. 51 (2012) 380-388; https://doi.org/10.1016/j.commatsci.2011.08.008

[5] Kaner R B, Gilman J J, Tolbert S H., Science, 2005, 308(5726):1268-1269; https://doi.org/10.1126/science.1109830

[6] Yuan Ren, Xuejie Liu, Xin Tan, Shiyang Sun, Huai Wei, Feng Lu, Applied Surface Science 298 (2014) 236-242; https://doi.org/10.1016/j.apsusc.2014.01.168

[7] Jian Yang, Pengfei Zhang, Yefei Zhou, Jing Guo, Xuejun Ren, Yulin Yang, Qingxiang Yang, Journal of Alloys and Compounds 556 (2013) 160-166; https://doi.org/10.1016/j.jallcom.2012.12.099

[8] B. Yang, X.H. Peng, H.G. Xiang, D.Q. Yin, C. Huang, S. Sun, T. Fu, Journal of Alloys and Compounds, 739 (2018) 431-438; https://doi.org/10.1016/j.jallcom.2017.12.240

[9] Schwarz K, Journal of Physics C: Solid State Physics, 1977, 10(2):195; https://doi.org/10.1088/0022-3719/10/2/007

[10] Huaizheng Zhang, Limin Liu, Shaoqing Wang, Acta Metallurgica Sinica, 2006(05):554-560.

[11] Yuan Ren, Qing Xia, Chao Zhang, Xuejie Liu, Zhi Li, Fucheng Zhang, Applied Surface Science 357 (2015) 1613-1618; https://doi.org/10.1016/j.apsusc.2015.10.045

[12] Liu W, Liu X, Zheng W T, et al., Surface Science, 2006, 600(2):257-264; https://doi.org/10.1016/j.susc.2005.10.035

[13] Yang J, Huang J H, Fan D Y, et al., Journal of Alloys and Compounds, 2016, 689:874-884; https://doi.org/10.1016/j.jallcom.2016.08.040

[14] Wang Haiyan, Mao Weimin, Gao Xueyun, Ren Huiping, Zhang Hongwei, Ansactions of Materialsand Heat Treatment, 2014, 35:201-204.

[15] Xiong H H, Zhang H H, Zhang H N, et al., Journal of Wuhan University of Technology-Mater. Sci. Ed, 2018, 33(5):1076-1081; https://doi.org/10.1007/s11595-018-1937-2

[16] Johansson S A, Christensen M, Wahnström G., Physical Review Letters, 2005, 95(22):226108; https://doi.org/10.1103/PhysRevLett.95.226108

[17] WEI S K, ZHENG S Q, XIE C, et al., Journal of Molecular Liquids, 2020, 319:114135; https://doi.org/10.1016/j.molliq.2020.114135

[18] Wang C, Dai Y B, Gao H Y, et al., Materials Transactions, 2010, 51(11):2005-2008; https://doi.org/10.2320/matertrans.M2010244

[19] Lv Yanan, Zhang Shunhu,Chen Dong, Iron Steel Vanadium Titanium, 2018, 39(05):162-166.

[20] Li Yunkuo. Hei Bei Tang Shan: North China University of Science and Technology, 2022.

[21] Xue F Y, Wang H Y, Zhao H, et al., Advanced Materials Research, 2011:174-177;

https://doi.org/10.4028/www.scientific.net/AMR.150-151.174

[22] Nakamura K, Yashima M., Materials Science and Engineering: B, 2008, 148(1-3):69-72; https://doi.org/10.1016/j.mseb.2007.09.040

[23] Tingaud D, Maugis P., Computational Materials Science, 2010, 49(1):60-63; https://doi.org/10.1016/j.commatsci.2010.04.020

[24] Jang J H, Lee C H, Heo Y U, et al., Acta Materialia, 2012, 60(1):208-217; https://doi.org/10.1016/j.actamat.2011.09.051

[25] Wang C W, Chong Yu, Applied Surface Science, 2009, 255(6):3669-3675; https://doi.org/10.1016/j.apsusc.2008.10.017

[26]Tengfei Li, Tianmo Liu, Hongmei Wei, Shahid Hussain, Jinxing Wang, Wen Zeng, Xianghe Peng, Zhongchang Wang, Applied Surface Science, 2015, 355: 1132-1135; https://doi.org/10.1016/j.apsusc.2015.07.189

[27] Lailei Wu, Yachun Wang, Zhigang Yan, Jingwu Zhang, Furen Xiao, Bo Liao, Journal of Alloys and Compounds,2013,561:220-227; https://doi.org/10.1016/j.jallcom.2013.01.200

[28] Baker R G. Precipitation processes in steels[J]. ISI Spec. Rep, 1959, 64:1.

[29] Bramfitt B L, Metallurgical Transactions, 1970, 1(7):1987-1995; https://doi.org/10.1007/BF02642799

[30] Zhu Liguagn, Wang Yan, Wang Shuoming, Zhang Qingjun, Iron and steel, 2019, 54:216-223.

[31] Wang Yan, HeiBei TangShan: North China University of Science and Technology, 2019.

[32] Nayak S S, Misra R D K, Hartmann J, et al., Materials Science and Engineering: A, 2008, 494(1-2):456-463; https://doi.org/10.1016/j.msea.2008.04.038